Supporting Information

Guo et al. 10.1073/pnas.1114781109

SI Text

Supporting Data. ***Identifying branches, cell protrusions, acinar attraction, and acinar extension.*** To identify branches and protrusions, we manually traced the periphery of a single cell or a multicell acinus, which was then used to compute the center of geometry O and the average distance $\langle r \rangle$ from O to cell periphery (Fig. S2*A*). A circle of radius $\langle r \rangle$ was drawn at O. A branch or protrusion (single- or multicell) was defined when a part of cell/acinar periphery was found continuously out of the circle with a certain amount larger than the root mean square deviation of r, i.e., $r \rangle \langle r \rangle + t \times \langle r^2 - \langle r \rangle^2 \rangle^{1/2}$, where t is the threshold (Fig. S2*A*). In this study, we have chosen $t = 1.5$, which was sufficient to exclude clusters that were not circular and should not be considered as branched.

Acinar attraction and acinar extension were defined manually by tracking the time-lapse data. Pairwise attraction was defined if there were only two acini moved to and coalesced with each other. Acinar extension was defined if a single acinus developed two branches pointing in opposite directions. The branches often pointed to other acini. At very high, unphysiological type I collagen concentration ([COL]) (2–4 mg/mL), acini/cells could develop branches without interactions with other acini/cells.

II. Examining if cells use soluble factors to induce direct branching. To examine if direct branching is induced by soluble factors secreted by cells when exposed to type I collagen (COL), we performed the following experiments. First, we examined if cells can secrete soluble factors to induce direct branching at distant cells through the medium [Fig. S3*B, Left* (red arrow)]. We prepared two chambers that were separated by a layer of agarose gel and shared the same medium. Each chamber was seeded with a layer of acini on the top of a basement membrane (BM) gel [ECM1 (Fig. S3*B, Left*)]. The density of acini was controlled around 30 ± 5.0 mm^{-2}. After 3 d, a gelification of another layer of ECM (ECM2, with [COL] (0.5 mg/mL) was performed on one of the chambers to induce direct branching. Here, the density of acini and collagen concentration in ECM2 were adjusted from Fig. 1*B, v* to ensure the formation of direct branching. After 3 d, the number of acini with direct branching was measured in each chamber [Fig. S3*B, Left* ("a," "b")]. The results suggest that branching acini cannot induce branching at nonbranched acini through the medium (Fig. S3*B, Right*).

Next, we examined if cells can secrete soluble factors to induce direct branching at distant cells and if the delivery of soluble factors occurs only through ECM [Fig. S3*C, Left* (red arrow)]. We prepared two layers of acini separated by a layer of BM gel (thickness: 300 ± 50 μm) (Fig. S3*C, Left*). The density of acini was controlled around 30 ± 5.0 mm^{-2}. After 3 d, the gelification of the second layer of ECM (ECM2, with [COL]): 0.5 mg/mL) was performed at the top of the upper layer of acini. Here, the density of acini and collagen concentration in ECM2 were adjusted from Fig. 1*B, v* to ensure the formation of direct branching. After 3 d, the number of acini with direct branching was measured at each layer [Fig. S3*C, Left* ("a," "b")]. The results suggest that branching acini cannot induce direct branching at nonbranched acini by secreting soluble factors through ECM that contains no COL (Fig. S3*C, Right*).

Finally, we examined the possibility that cells can secrete soluble factors to induce direct branching at distant cells, but the delivery of soluble factors occurs only through ECM that contains COL [Fig. S3*D, Left* (red arrow)]. We prepared a layer of dilute acini (densities < 10 mm^{-2}) on the top of a BM gel (ECM1, Fig. S3*D, Left*), followed by the gelification of the second layer of ECM (ECM2, with [COL] = 0.5 mg/mL and thickness: 300 ± 50 μm). Here, the low density of acini was adjusted from Fig. 1*B, v* to ensure no direct-branching formation. After 3 d, a layer of single cells (density > 50 mm^{-2}) was seeded on the top of ECM2. The high density of single cells was adjusted from Fig. S2*G* to ensure the formation of direct branching. After 3 d, the number of acini with direct branching was computed at each layer [Fig. S3*D, Left* ("a," "b")]. The results suggest that branching cells cannot induce direct branching at nonbranched acini by secreting soluble factors through ECM that contains COL (Fig. S3*D, Right*). Represented outcomes of "a" and "b" were demonstrated in Fig. S3*D, Center*.

Defining the central and peripheral regions in the transmission of traction force. To define the central region in Fig. 3 and Fig. S5*B*, we first identified a central line M connecting the geometrical centers of two interacting acini or cell clusters. We noted that cell branching primarily occurred along the central line M (Fig. 1*B,i*). We also found that during the early stage of acinar interactions (1–6 h, the period in which we computed the correlations between cell motions and ECM deformations), the tips of branches were often led by a single cell with width ∼10–20 μm. We therefore used M to define a box (of a height of 20 μm, hereafter referred to as the central region) that enclosed the two outer layers (proximal to each other) of cells at the two acini or cell clusters [Fig. 3*B, i* (dotted cyan lines)]. The motions of branched cells were used to obtain the histograms of Fig. 3*B, ii* and Fig. S5*B*. To define the peripheral regions, two boxes with a height of 20 μm were drawn right above and below the central region [Fig. 3*B, ii* (dotted cyan and pink lines)]. The height of the boxes was set based on the average size of a single cell. The motions of the cells enclosed by the central region were used to compute the alignments between cells and ECM (in the central or the peripheral regions).

Measuring cell and ECM motions. To track cell motions, the geometrical center of a cell nucleus (indicated by H2B-cerulean) was monitored. To track ECM deformation, fluorescent beads (diameter: 1 μm) were embedded in ECM2 or conjugated with ECM2 through anti-COL antibodies. Alternatively, ECM2 (containing COL) was treated with anti-COL antibody and fluorescent bead-conjugated secondary antibody (diameter: 1 μm) to ensure that the observed displacement of beads occurred along COL fibers. Images of beads within 20 μm (the average size of single cells) above and below the focal plane of acini were taken to analyze ECM deformation.

Computing the alignment between cell motions and ECM deformations. The motions of cells at the boundaries of the central region were used as the reference to compute the alignment between cells motions and ECM deformations. For [COL] = 0, 0.3, 0.5, and 1 mg/mL, we find that the average motility of cells was approximately 0.2 ± 0.05 μm/min (mean ± SEM, $N = 100$ for each [COL]) without an explicit dependence on [COL].We then set the half of the average cell motility (i.e., 0.1 μm/min) as the threshold to compute the alignment effect. For any event of cell motion ($\vec{V}_c$) at a time interval ($\Delta\tau$), if $|\vec{V}_c| \geq 0.1$ μm/min, we used $\vec{V}_c$ as the reference to compute the alignment effect. Specifically, the movements of all the beads within the central region ($\vec{V}_E$) and the peripheral regions ($\vec{V}_E'$) would be used to compute the inner product, $\vec{V}_c \cdot \vec{V}_E$ and $\vec{V}_c \cdot \vec{V}_E'$. We then used these inner products to represent the alignments between cell motions and

ECM deformations in the central (peripheral) region(s). The number of sample, $N = 10 \times 10 \times 10$ [(the number of cells) × (the number of beads) × (the number of events)], for all the histograms.

Confirming force transmission along COL fibers. To examine whether the direct transmission of force occurs along COL fibers, ECM2 ([COL] = 0.5 mg/mL) was conjugated with fluorescent beads through anti-COL antibody after gelling on acinus/cell-free ECM1. Cells (approximately 100 cells/mm^2) were then seeded on ECM2 (i.e., no acini/cells between ECM1 and ECM2). Here, the density of cells was adjusted from Fig. S1*G* to ensure the formation of direct branching. Time-lapse microscopy revealed that cells did develop direct branching on ECM2 (Fig. S5*A*). Moreover, the motions of beads exhibited similar patterns as those shown in Fig. 3*B, ii* (Fig. S5*B*). Thus, the results in Fig. 3*B, ii* were correlated with the transmission of forces along COL fibers. These data suggest that COL fibers mediate direct transmission of forces.

Defining the stability of linear patterns in rectangular cell traps. After ECM2 gelled on the top of the engineered rectangular cell traps (Fig. 6*A*), the sparsely seeded cells (30–50% of the trap space) formed aggregates through COL fibers. To define globular and tubule-like structures, we identified the two principal axes (x' and y') of individual cell aggregates after 30 h of ECM2 gelification. The width along each axis, L'_x and L'_y, were measured (Fig. S6*A*). To discard single cells and small clusters, only aggregates with L'_x or $L'_y \geq 100$ μm were considered. We defined the final aspect ratio of the cell cluster as L'_y/L'_x, whereas its initial aspect ratio was defined by the dimension of cell trap as L_y/L_x. Here, x and y axes represent the coordinates for the traps (Fig. 6*A*). If $L'_y/L'_x < L_y/L_x$, we defined that the linear patterns were not stable [cell clusters often collapsed into globular structures (Fig. S6*A, Top*)]. On the other hand, if $L'_y/L'_x \geq L_y/L_x$, we defined that the linear patterns were stable [cell clusters often extended into tubule-like structures (Fig. S6*A, Bottom*)]. We found that globular collapse and tubular expansion were mutually exclusive. In addition, they possessed bistability and exhibited an all-or-none behavior. The measurements of initial and final aspect ratios are shown in Fig. S6*B*.

The influences of known morphogens on COL-induced direct branching. To see if TGFβ1/EGF treatment or PI3K/Rac1 inhibition affects the initiation of direct branching, cells were seeded on BM gels (ECM1) for 72 h to form acini, followed by the overlay of ECM2 ([COL] = 0.5 mg/mL) in serum-free, growth-factor-free medium (to minimize interference from other known biochemical stimulations) containing various chemicals. These chemicals included inhibitory TGFβ1 [5 ng/mL, which is known to suppress branching morphogenesis (1)], EGF (100 ng/mL), Rac1 inhibitor (NSC2376, 70 μM), and PI3K inhibitor (LY294002, 20 μM). To see if direct branching required ERK1, ERK1 inhibitor (PD98095, 10 μM) has also been tested. After ECM2 overlay for 24 h, the frequency of directed branching at individual acini was measured.

To see if TGFβ1/EGF treatment or PI3K/Rac1/ERK1 inhibition affects the maintenance of direct branching, acini on BM gels (ECM1) were covered by ECM2 ([COL] = 0.5 mg/mL) for 48 h to facilitate branching formation. The system was then perfused with serum-free, growth-factor-free medium containing TGFβ1 (5 ng/mL), EGF (100 ng/mL), Rac1 inhibitor (NSC2376, 70 μM), PI3K inhibitor (LY294002, 20 μM), or ERK1 inhibitor (PD98095, 10 μM).

Supporting Experimental Procedures. ***Materials and Methods. Cell culture and cell line preparation.*** MCF-10A cells were kindly provided by Anand Asthagiri (Chemical Engineering, California Institute of Technology). Cells were maintained in DMEM/Ham's F-12 containing Hepes, L-glutamine, 5% (vol/vol) horse serum (Invitrogen-Gibco), 20 ng/mL EGF (Peprotech), 0.5 μg/mL hydrocortisone (Sigma-Aldrich), 0.1 μg/mL cholera toxin (Sigma-Aldrich), 10 μg/mL insulin (Sigma-Aldrich), and 1% penicillin/streptomycin.

Lentivirus encoding CFP-conjugated histone H2B (H2B-cerulean) or mCherry [both under human phosphoglycerate kinase (PGK) promoter] were gifts from Rusty Lansford and David Huss (Biology, California Institute of Technology) (2). To engineer cells expressing both H2B-cerulean and mCherry, we first developed stable cell line expressing H2B-cerulean. Cells at 20–30% confluency were infected with lentivirus encoding H2B-cerulean. The infected cells were then repetitively diluted in 96-well plates to enable the selection and expansion of single fluorescent colonies. We then infected stable H2B-cerulean-expressed cells with lentivirus encoding mCherry to develop cell line expressing H2B-cerulean in the nucleus and mCherry throughout the entire cytoplasm.

Yes-associated protein (YAP)-overexpressing MCF-10A cells and YAP-KO MCF-10A cells were generous gifts from Kun-Liang Guan at University of California, San Diego.

Reagents. The Rho-kinase inhibitor Y-27632, the ERK/MAPK inhibitor PD 098059, the PI3K inhibitor LY294002, and mouse monoclonal anticollagen type I primary antibodies were purchased from Sigma. The FITC-conjugated type I collagen was purchased from AnaSpec Inc. The Rac1 inhibitor 553502 (NSC23766) was obtained from Calbiochem. Rabbit polyclonal antiphosphorylated FAK (at tyrosine 397) and antiphosphorylated MLC (at serine 19) antibodies were purchased from Santa Cruz Biotechnology. Rabbit polyclonal anti-YAP antibody was a gift from Kun-Liang Guan (University of California, San Diego). Fluorescent beads coated with anti-mouse secondary antibodies were generous gifts from Anand Asthagiri (California Institute of Technology). BD Matrigel (with total proteins: 8–10 mg/mL) and 3D Culture Matrix Rat Collagen I (5 mg/mL) were purchased from BD Biosciences and R&D Systems, respectively. Pacific Blue or FITC-conjugated goat anti-rabbit and mouse IgGs, and fluorescent beads of various colors and sizes (0.2 μm–10 μm) were purchased from Invitrogen.

Immuno-staining. Cell samples were fixed in 4% paraformaldehyde for 15 min, and permeabilized with 0.1% Triton X-100 for 20 min at room temperature (RT). The cells were then incubated with rabbit polyclonal antiphosphorylated FAK (at tyrosine 397), antiphosphorylated MLC (at serine 19), or anti-YAP antibodies overnight at 4 °C, followed by incubation with goat secondary antibody conjugated with Pacific Blue (410/455 nm) or FITC for 2 h at RT.

Perfusion chambers. To assemble the chambers for live cell imaging, we fabricated stainless steel plates with a hole in their middle; the size and the shape of the hole was designed to match the size and the shape of the coverslip. We used nail polish to seal the coverslip at the bottom of the plate. To perform perfusion experiments, we prepared a polydimethylsiloxane (PDMS) block to seal the top of the chamber. Before sealing, two open channels of a diameter of 1 mm were punched at the PDMS block to allow for the insertion of tubes. One tube was for the perfusion of medium (normal medium or serum-free, growth-factor-free medium with specific pharmacological reagents) buffered with 5% CO_2 delivered through a humidifier. The other was for the delivery of the wasted medium to a sink. Silicone rubber aquarium sealant was used to seal the PDMS block with the chamber. After the sealant was dry and the chamber was stabilized, we filled the chamber with perfusion medium and used gravity to maintain the perfusion at a flow rate of approximately 10–100 μL/min.

3D gel preparation and rigidity measurement. In our two-step 3D ECM preparation, the first layer of ECM (ECM1) is BM gels, whereas the second layer (ECM2) is a mixture of COL and BM components. We prepared the BM gels following the protocol provided by the manufacturer. The total concentration of proteins in original growth factors-reduced (GFR) BD Matrigel stock solution is 8–10 mg/mL. The major components are laminin (approximately 61%), collagen IV (approximately 30%) and Entactin (approximately 7%). To make BM gels, we first prepared perfusion chambers sealed with coverslips on the bottom. The stock solution (100%) of BD Matrigel (stored at 4 °C) was then spread onto the top of the coverslips (80–120 $\mu l/cm^2$) at 37 °C for 20–30 min. This allowed the stock solution to form a layer of gel with a variable height (200–400 μm). At the same time, we prepared medium (normal medium or serum-free, growth-factor-free medium with specific pharmacological reagents) containing 2% soluble BM (20 μL of BD Matrigel solution per 1 mL of medium) at 4 °C. After the gels formed, individual MCF-10A cells at various densities were seeded on the top of BM gels, followed by the coverage of culture medium containing 2% BM. We then placed the chamber in a 37 °C incubator and changed the medium every 3 d.

To prepare the second layer of ECM (ECM2), we first prepared COL solutions at 1–1.3 mg/mL from the stock solution. Following the protocol provided by the manufacturer, we mixed the stock solution of COL (5 mg/mL in 20 mM acetic acid), 10 × PBS, 7.5% sodium bicarbonate ($NaHCO_3$), and water (ddH_2O) to a final concentration of COL 1–1.3 mg/mL in 1 × PBS, neutralized to pH = 7 by 7.5% $NaHCO_3$. According to our measurement, the volume ratio of the required amount of collagen stock solution and 7.5% $NaHCO_3$ is 5 : 1. We then mixed the BM stock solution and the COL solutions at various ratios to obtain ECM2 solutions with collagen concentration ranging from 0 to 1 mg/mL and rigidity within 170 ± 40 Pa.

To finalize the 3D environment, medium over the acini was carefully removed, followed by the gelification of ECM2 on the top of acini. After the gel formed (at 37 °C for 20–30 min), medium (normal medium, or serum-free, growth-factor-free medium with specific pharmacological reagents) was added to fill the chamber.

For all the gels prepared, we characterized ECM rigidity by a compression test (3, 4) and measured the Young's modulus through the corresponding stress-strain curve.

Two-step 3D ECM construction. Individual cells at various densities were plated on BM gels ([ECM1 (Fig. 1*A*) with rigidity approximately 175 Pa comparable to the physiological one] and covered by medium containing 2% BM. After 3 d, cells formed acini surrounded by assembled BM (5). The 3D environment was then completed by having another layer of ECM [ECM2 (Fig. 1*A*)] gelling on top. To create different ECM structures, COL was mixed with BM at various ratios in ECM2. The amount of COL and BM in ECM2 was adjusted to create a similar rigidity as ECM1. For example, ECM2 containing 1–1.3 mg/mL COL without any BM has a similar rigidity to ECM1 containing 100% BM without any COL (6). Overall, a series of ECM2 were created with [COL] ranging from 0 to 1 mg/mL, while their rigidity was maintained within 170 ± 40 Pa.

Micro-patterned cell traps. To specify the initial size and geometry of multicell clusters in COL-induced branching, we used a protocol modified from the one developed by Nelson et al. (7). We used PDMS stamps to generate cell traps in agarose gels. For circular traps, PDMS stamps were created by soft lithography with a circular shape of a diameter of 200 μm and a height of 100 μm. Each circular trap was separated by a distance varying from 200 to 1,000 μm. Likewise, to create rectangular traps, PDMS stamps were created with a rectangular shape of a height of 100 μm, a width of 200 μm, and various lengths ranging from 200 to 2,000 μm. Each rectangular trap was separated by a distance 500 μm.

To create the traps, 2% agarose premixed with 1% gelatin was boiled and filled in perfusion chambers. Here, we used gelatin to enhance cell trapping (the amount of gelatin used here does not induce branching). A PDMS stamp was placed on the top of the boiled agarose and gelatin mixture. The chamber was then left in 4 °C for 1 h. After the gel formed, we removed the stamps and filled the traps with MCF-10A cells. Excessive cells were washed away and the chamber was filled with normal or serum-free, growth-factir-free medium. The chamber was then mounted to a microscope stage for time-lapse microscopy. After 15–30 min, the medium was replaced by a solution of BM and COL mixture (at various ratios) to form a layer of gel on the top of the trapped cell clusters. Once the gel formed, we sealed the chamber and perfused it with normal or serum-free, growth-factor-free medium, and resumed the time-lapse microscopy to trace the induction of branching.

Microscopy for live cell imaging. An Olympus IX71 equipped with automatic XYZ stages (MS-2000, ASI) and piezo-electric objective stages (P-721 Pifoc, Physik Instrumente) were used for multiposition, z-scanning, and auto-focusing time-lapse epifluorescence/scanning microscopy. An environmental chamber was used to maintained humidity, CO_2 concentration (5%), and temperature (37 °C). For phase-contrast and/or epifluorescent microscopy, the microscope was equipped with motorized excitation and emission filters with a shutter control (lambda 10-3, Sutter), an electron-multiplying CCD camera (ImagEM, C9100-13, Hamamatsu, 512 × 512 pixels, water-cooled to −95 °C), and a 120 W fluorescent illumination lamp (X-CITE 120Q, EXFO). For two-photon scanning microscopy, the microscope was equipped with multiwavelength lasers (Spectral Physics) and photomultiplier tubes (H10425 and H7422-40, Hamamatsu). All microscopies were performed using 40 × phase contrast (N.A.: 0.75, Olympus), 20 × (N.A.: 0.45, Olympus), or 10 × (N.A.: 0.3, Olympus) objectives. For phase-contrast and/or epifluorescence time-lapse microscopy, Metamorph (version 7.7) was used to control the devices and the image acquisition. For scanning microscopy, Labview was used to run automatic scanning and image acquisition. The exposure time and gains were adjusted according to image quality and the photo-bleaching effect.

Image processing and analysis. All the image data were acquired by Metamorph (version 7.7) or Labview programs and analyzed by Metamorph, Matlab, and ImageJ. The band-pass Fourier transforms (ImageJ) were performed to enhance the visualization of cell nucleus (H2B-cerulean). The filters were selected based on the size of the nucleus.

1. Soriano JV, Orci L, Montesano R (1996) TGF-beta1 induces morphogenesis of branching cords by cloned mammary epithelial cells at subpicomolar concentrations. *Biochem Biophys Res Commun* 220:879–885.
2. Sato Y, et al. (2010) Dynamic analysis of vascular morphogenesis using transgenic quail embryos. (Translated from English) *PLoS One* 5:e12674 (in English).
3. Zent R, et al. (2001) Involvement of laminin binding integrins and laminin-5 in branching morphogenesis of the ureteric bud during kidney development. *Dev Biol* 238:289–302.
4. Maskarinec SA, Franck C, Tirrell DA,Ravichandran G (2009) Quantifying cellular traction forces in three dimensions. *Proc Natl Acad Sci USA* 106:22108–22113.
5. Muthuswamy SK, Li D, Lelievre S, Bissell MJ,Brugge JS (2001) ErbB2, but not ErbB1, reinitiates proliferation and induces luminal repopulation in epithelial acini. *Nat Cell Biol* 3:785–792.
6. Paszek MJ, et al. (2005) Tensional homeostasis and the malignant phenotype. *Cancer Cell* 8:241–254.
7. Nelson CM, Vanduijn MM, Inman JL, Fletcher DA, Bissell MJ (2006) Tissue geometry determines sites of mammary branching morphogenesis in organotypic cultures. *Science* 314:298–300.

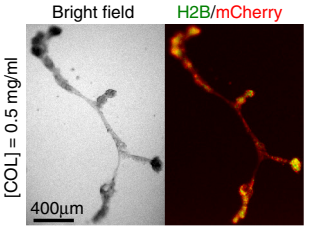

Fig. S1. Represented long-scaled tubular patterns occurred after long-term culture. Cells were grown into acini, followed by the overlay of ECM2 containing [COL] = 0.5 mg/mL for 5 d. Initial acinus density (c_{acinus}) before ECM2 gelification: 30 ± 5 mm^{-2}. Green: H2B-cerulean at cell nucleus. Red: mCherry expressed in the whole cell.

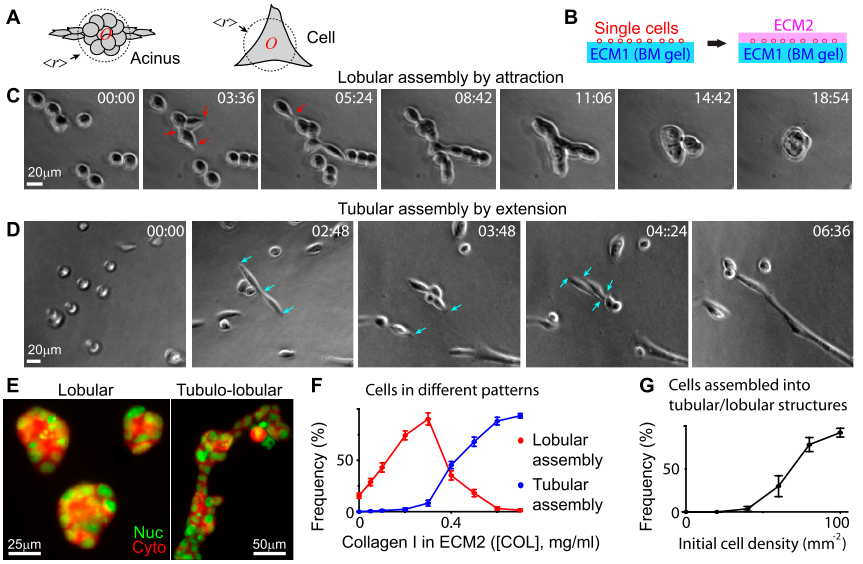

Fig. S2. Preexisting acinus was not required for branching pattern formation. (*A*) Diagram to show the definition of the geometrical center (*O*), the average distance $\langle r \rangle$ from *O* to the periphery of the acinus (*Left*) or of the single cell (*Right*). Branches and protrusions are defined in the region outside of the circle (dotted line) of radius $\langle r \rangle$ with an amount $\rangle \langle r \rangle + t \times \langle r^2 - \langle r \rangle^2 \rangle^{1/2}$, where t is the threshold (see *SI Text*). In this study, we have chosen $t = 1.5$. (*B*) The experimental setup. Single cells were seeded on BM gels (ECM1), immediately followed by the gelification of another layer of ECM (ECM2) on top. (*C*) Represented images of globular assembly from single cells when ECM2 is rich of BM. Red arrows indicate polarized branching formation at individual cells. (*D*) Represented images of tubular assembly from single cells when ECM2 contains intermediate to high levels of COL. Cyan arrows indicate bipolar branching formation at individual cells. (*E*) Represented globular (*Left*) and tubulo-globular (*Right*) structures formed through single cell assembly. Nucleus (Nuc) indicated by the fluorescence of H2B-CFP. Cytoplasm (Cyto) indicated by the fluorescence of mCherry expressed throughout the whole cell. To enhance visualization, background scattering from the ECM gels was removed. (*F*) The frequency of individual cells ($N = 200$) in different patterns in response to the change of COL concentration in ECM2 ([COL]). Initial cell density: 90 ± 5 mm^{-2}. (*G*) The frequency of individual cells being assembled into globular or tubular structures with different initial cell densities (before ECM2 overlay). COL in ECM2 ([COL]): 0.5 mg/mL. In *C* and *D*, time is in hours and minutes, and scale bar is 20 μm. In *F* and *G*, data are represented in mean ± SEM.

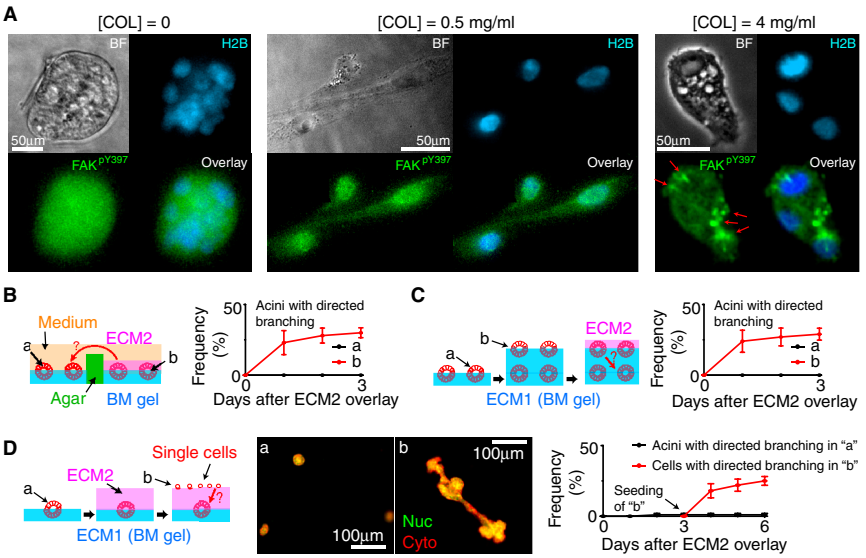

Fig. S3. Direct branching was unlikely to be induced by FAK up-regulation or diffusible factors secreted by branched cells. (*A*) Immuno-staining of FAK^{pY397}. (*Left*) Acinus overlaid with ECM2 containing 100% BM and no COL. (*Center*) Cell branching induced by ECM2 containing 0.5 mg/mL COL. (*Right*) Cells seeded on rigid COL gels (4 mg/mL) as the positive control. Red arrows indicated localized FAK^{pY397} signals. Scale bar: 50 μm. H2B: H2B-cerulean. Overlay: H2B (cyan) and FAK^{pY397} (green). BF, bright field. (*B–D*) Experimental setup and results to examine if cells secrete soluble factors to induce direct branching at distant cells. *Left* of (*B–D*) Experimental setups to examine if cells secrete soluble factors to induce direct branching at distant cells through (*B*) the medium or (*C–D*) the ECM. See *SI Text* for more details. *Right* of (*B–D*) Frequencies of individual acini (and cells in *D*) developing direct branching in the "a" and "b" populations in each experiment. *Center* of (*D*) Represented images of the outcomes of "a" and "b" in the experimental setup of (*D*). Scale bar: 100 μm. Nucleus (Nuc) indicated by the fluorescence of H2B-CFP. Cytoplasm (Cyto) indicated by mCherry expressed throughout the whole cell. In *B–D*, Data are represented in mean ± SEM.

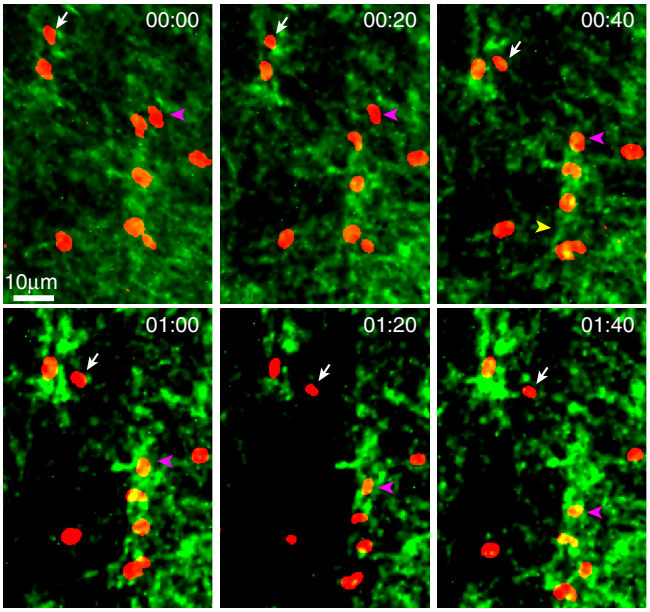

Fig. S4. Second harmonic generation (SHG) of COL showed random initial orientations of COL fibers in self-assembled ECM. COL gels (1 mg/mL) was generated and placed under multiphoton scanning microscope to examine the distribution and the orientations of COL fibers at a single focal plane. The images were collected through SHG (green in the images, laser wavelength: 800 nm). To see how cells moved on COL gels, cells were spread on the gel and cell nuclei were imaged through H2B-cerulean (red in the images). Two examples of cell motions were indicated (white arrow and pink arrowhead). Time is in hours and minutes. Microscope objective: 20 × (water immersed, N.A. = 0.95, Olympus).

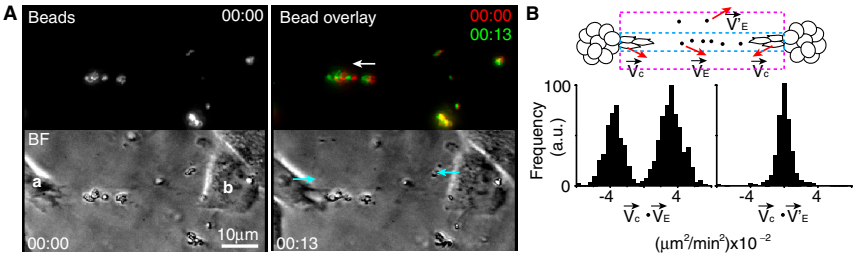

Fig. S5. Direct branching involved a direct transmission of traction force along COL fibers. (*A*) Represented images of cell motions and ECM deformation (indicated by fluorescent bead-conjugated type I collagen antibodies). Cyan arrows indicate the movements of cells (labeled by "a" and "b" at $t = 00:00$). Bead overlay: overlay of fluorescent images of beads at the earlier time (red) and at the later time (green). White arrows indicate bead displacements. Time is in hours and minutes. BF, bright field. (*B*) (*Upper*) Diagram to show the central and peripheral regions between two interacting cell clusters. $\vec{V}_c$: cell motion.$\vec{V}_E(\vec{V}'_E)$: bead motion In the central (peripheral) region. (*Lower*) Histograms of alignments between the motions of cells (*Left*) at the central region and (*Right*) at the peripheral regions. Data were obtained after seeding cells for 24 h on fluorescent beads coated with ECM2 ([COL] = 0.5 mg/mL). Only cells within the central region (dotted cyan box) were used to compute the correlations. $N = 1,000$ (cells × beads × events) and the frequency is normalized to the maximum in each histogram.

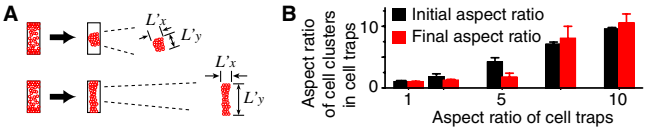

Fig. S6. System spatial anisotropy affected the stability of linear patterns. (*A*) The definition of globular and tubule-like structures in rectangular cell traps. (*Upper*) The formation of globular structures. After 30 h of ECM2 gelification, the principal axes of cell clusters were identified and the width along each axis was measured (i.e., L'_x and L'_y). Cell clusters were defined to have a globular collapse if the final aspect ratio (L'_y/L'_x) is less than the initial one (L_y/L_x, defined by the dimension of traps). (*Lower*) Cell clusters were defined to have a tubular expansion if $L'_y/L'_x > L_y/L_x$. (*B*) The initial (black) and final (red, after 30 h of ECM2 gelification) aspect ratios of cell clusters within individual traps in response to changes of aspect ratio of the traps ($N = 20$ and $L_x = 200$ μm for each case). Data are represented in mean ± SEM.

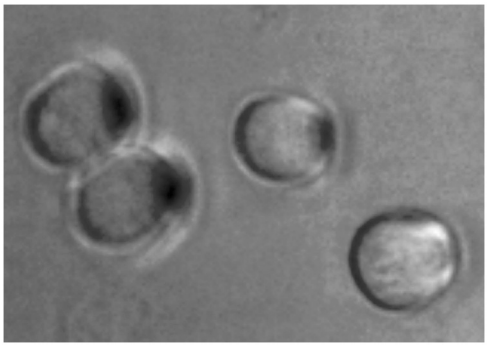

Movie S1. Time-lapse movie of Fig. 1*B*. MCF-10A cells were seeded on BM gels (100% BD Matrigel, ECM1) to form acini, followed by the gelification of another layer of ECM (ECM2) on top. Here, ECM2 contained no COL. [COL] in ECM2. Time interval between each frame: 8 min.

Movie S1 (AVI)

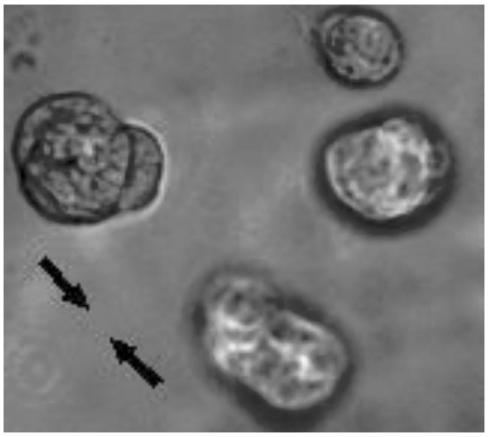

Movie S2. Time-lapse movie of Fig. 1*C*. MCF-10A cells were seeded on BM gels (100% BD Matrigel, ECM1) to form acini, followed by the gelification of another layer of ECM (ECM2) on top. ECM2 is a mixture of COL and BM to ensure a constant rigidity as ECM1. [COL] in ECM2. Here, $[\mathrm{COL}] = 0.3$ mg/mL. The development of direct branching (i.e., acini moving to each other) is labeled by black arrow. Time interval between each frame: 8 min.

Movie S2 (AVI)

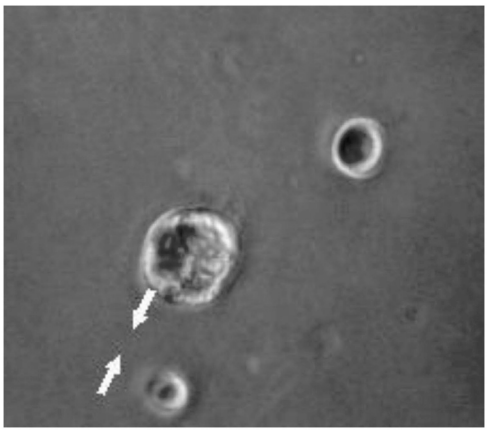

Movie S3. Time-lapse movie of Fig. 1*D*. MCF-10A cells were seeded on BM gels (100% BD Matrigel, ECM1) to form acini, followed by the gelification of another layer of ECM (ECM2) on top. ECM2 is a mixture of COL and BM to ensure a constant rigidity as ECM1. [COL] in ECM2. Here, $[\mathrm{COL}] = 0.5$ mg/mL. The development of direct and induced branching is labeled by white arrow. Time interval between each frame: 7 min.

Movie S3 (AVI)

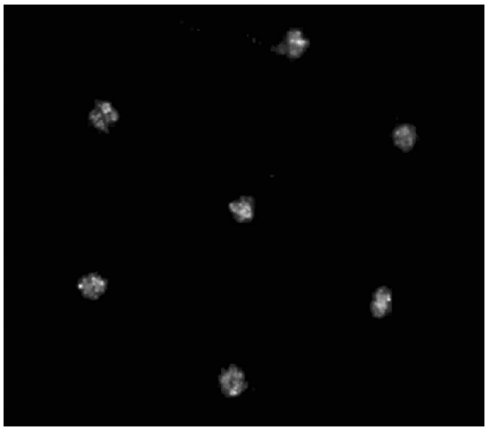

Movie S4. Time-lapse movie for the no-branching pattern in circular trap experiment. Circular cell traps in agarose gels were created by PDMS stamps with a fixed diameter $l = 200$ μm and a fixed intertrap distance $\lambda = 600$ μm. Cells were seeded in the traps, followed by the gelification of ECM2 on top. Here the concentration of COL in ECM2 ($[\mathrm{COL}]$) = 0.1 mg/mL. Time interval between each frame: 10 min. No branching pattern was found throughout the entire imaging course (approximately 36 h).

Movie S4 (AVI)

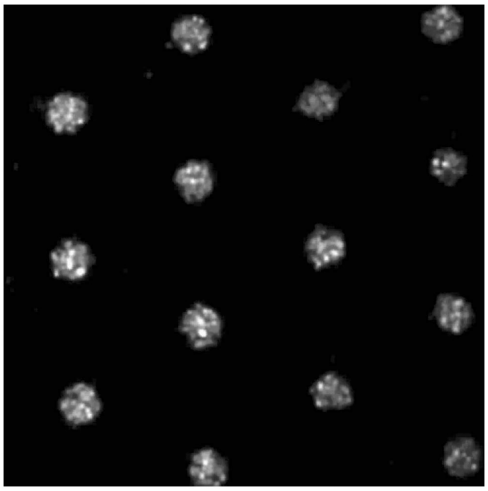

Movie S5. Time-lapse movie for the direct-branching (pairwise branching) pattern in circular trap experiment. Circular cell traps in agarose gels were created by PDMS stamps with a fixed diameter $l = 200$ μm and a fixed intertrap distance $\lambda = 400$ μm. Cells were seeded in the traps, followed by the gelification of ECM2 on top. Here the concentration of COL in ECM2 ($[\mathrm{COL}]$) = 0.2 mg/mL. Time interval between each frame: 10 min. The development of direct branching between adjacent cell traps is labeled by white arrow.

Movie S5 (AVI)

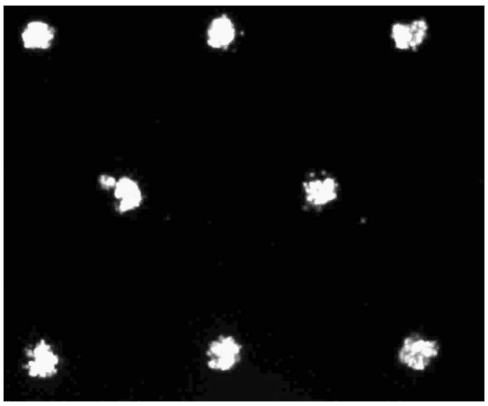

Movie S6. Time-lapse movie for the direct-branching (multipaired branching) pattern in circular trap experiment. Circular cell traps in agarose gels were created by PDMS stamps with a fixed diameter $l = 200$ μm and a fixed intertrap distance $\lambda = 600$ μm. Cells were seeded in the traps, followed by the gelification of ECM2 on top. Here the concentration of COL in ECM2 $([\mathrm{COL}]) = 0.3$ mg/mL. Time interval between each frame: 10 min. The development of direct branching between adjacent cell traps is labeled by white arrow. Note the formation of multipaired branching.

Movie S6 (AVI)

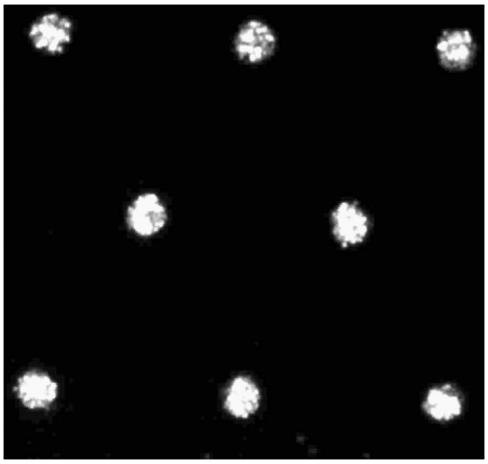

Movie S7. Time-lapse movie for the random-branching pattern in circular trap experiment. Circular cell traps in agarose gels were created by PDMS stamps with a fixed diameter $l = 200$ μm and a fixed intertrap distance $\lambda = 600$ μm. Cells were seeded in the traps, followed by the gelification of ECM2 on top. Here the concentration of COL in ECM2 $([\mathrm{COL}]) = 0.5$ mg/mL. Time interval between each frame: 10 min. Note that cells in each trap developed more than six branches.

Movie S7 (AVI)